Raman microprobe scattering of solid silicon and germanium at the melting temperature

Hua Tang and Irving P. Herman
Department of Applied Physics, Columbia University, New York, New York 10027
(Received 27 July 1990; revised manuscript received 20 September 1990)

Raman microprobe spectroscopy is used to study *c*-Si and *c*-Ge heated to the melting point by a tightly focused cw laser beam. At their respective melting temperatures, the Raman shifts of solid Si and Ge are 481.7±0.4 and 281.4±0.5 cm^{-1}, and the linewidths are 24.3±0.3 and 14.1±0.5 cm^{-1}. Optical-phonon coupling both to two and to three phonons is necessary to explain the Raman linewidths measured here at the melting temperature and those measured elsewhere at lower temperatures. Coupling to two phonons is important in determining anharmonic corrections to the Raman energy shift, while coupling to three phonons of lower energy is relatively less important. Polarization analysis of the Raman spectra has been used to differentiate the contributions from partially melted and nonmelted regions.

I. INTRODUCTION

The temperature dependence of first-order Raman scattering by phonons in silicon and germanium has been investigated extensively.[1–6] With increasing temperature, the Raman shift decreases and the linewidth increases in both semiconductors because of anharmonic effects.[1,2] Using this temperature dependence, Raman spectroscopy has been used to probe the temperature profile of conventionally heated[1,2] and laser-heated silicon,[4] sometimes with submicrometer resolution.[7] Raman analysis of semiconductors over a wide range of temperatures, up to melting temperature, is needed to better understand the contributions of volume expansion and anharmonic intermode coupling to the Raman shift and linewidth. For example, there are questions about the relative importance of cubic and quartic anharmonic terms in the potential for Raman scattering at high temperature. Apparently, only one Raman study of these semiconductors has been conducted at the melting point. A CO_2 laser was used to heat silicon films on quartz to form coexisting solid and liquid regions at the melting temperature.[8] Raman scattering was performed with mode-locked Ar-ion laser pulses and gated detection to filter out blackbody radiation. In this work, Raman microprobe analysis is used to probe Ar-ion laser-heated micrometer-dimension regions in bulk *c*-Si and *c*-Ge to analyze optical phonons in the solid phase at the melting temperature.

The coexisting solid and liquid phases in silicon formed by high laser power heating have been examined by several groups.[9–14] Complicated stable or time-varying structures, sometimes with solid or liquid lamellae, or grating-type structures, have been observed for relatively large (~40–500 μm diam) partially molten regions. Stable patterns were seen using CO_2 laser heating, with solid lamellae as narrow as 3 μm wide, while time-varying patterns were observed when a laser at shorter wavelength, such as an Ar-ion laser, was used for heating.[11] The coupling of light to the partially molten regions is complex because the reflectivity of the molten region is higher than that of the solid region. Analogous mixed solid-liquid regions are expected for the micrometer-dimension heated spots examined here in silicon and germanium.

II. EXPERIMENTAL PROCEDURE AND RESULTS

A linearly polarized cw Ar-ion laser (5145 Å) was focused to a 0.8-μm spot size (half-width of intensity decrease to $1/e$) onto the semiconductor sample, which was mounted in an evacuated vacuum chamber (10^{-4} Torr). The focused laser beam heated the sample and also provided photons for the spontaneous Raman spectrum. The backscattered Stokes Raman signal was transmitted through a rotatable $\lambda/2$ wave plate, followed by a beam splitter that transmitted light that was linearly polarized in only one direction. This polarization-analyzed Raman signal was measured by the detection system, consisting of a triple spectrometer and an intensified diode array. Laser-heated *c*-Si(001) and *c*-Ge(001) wafers were examined in $z(x,y)\bar{z}$ and $z(x,x)\bar{z}$ orientations, where x,y are the crystal [100] and [010] directions and x is also the laser polarization direction. Usually time-resolved Raman spectra were taken.

With laser power P below that needed for melting, Raman signals were observed with $z(x,y)\bar{z}$ orientation for Si and Ge but not with $z(x,x)\bar{z}$, as is expected.[15] Si melted for laser powers $P > 0.4$ W, while Ge melted for $P > 0.14$ W. The onset of melting was noted by changes in the Raman spectrum[16] and by the characteristic large-angle, swirling nature of the reflection pattern. Typical Raman spectra are shown in Fig. 1, for Si with $P = 1.2$ W. There are two peaks in the $z(x,y)\bar{z}$ spectrum, at 508.4 and 484.4 cm^{-1} when fit as Lorentzians, and only one peak in the $z(x,x)\bar{z}$ spectrum, at 481.3 cm^{-1}. When the asymmetric line shape of the higher-energy $z(x,y)\bar{z}$ peak is used in the fit, the lower-energy $z(x,y)\bar{z}$ peak coincides with the $z(x,x)\bar{z}$ feature. Raman spectra were integrated only for the first 0.5 sec of illumination for Si, because there was a

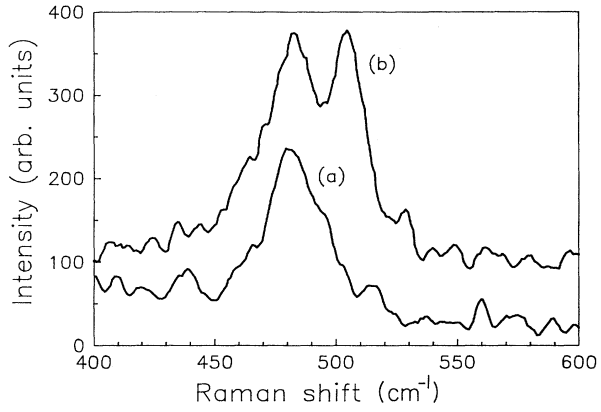

FIG. 1. Raman spectra of partially molten Si averaged for the first 0.5 sec of sample heating using a laser power of 1.2 W at 514.5 nm. For $z(x,x)\bar{z}$ analysis (a), only one peak is seen at 481.3 cm^{-1}, while for $z(x,y)\bar{z}$ Raman analysis (b), two peaks are observed at 508.4 and 484.4 cm^{-1} (Lorentzian fit), respectively.

flow of molten silicon for longer times. Longer integration times were possible for germanium.

The $z(x,x)\bar{z}$ peak in the Si spectra is at 481.7±0.4 cm^{-1} for $P=0.9-1.8$ W. In Ge, the peak is at 281.4±0.5 cm^{-1} for $P=0.16-0.70$ W. The linewidths [full width at half maximum (FWHM)] in these experimental regions are 24.3±0.3 cm^{-1} for Si and 14.1±0.5 cm^{-1} for Ge, and are corrected for instrumental resolution. Using atomic line sources, the instrumental response was found to closely approximate a Gaussian with a 2.5 cm^{-1} FWHM. This line shape was convoluted with the assumed Lorentzian Raman profile.

The intensity of the $z(x,x)\bar{z}$ Raman signal decreases slowly in partially molten Si and very quickly in Ge with increasing laser power. No Raman signal was seen in Ge for $P>0.7$ W.

III. DISCUSSION

When melting occurs, initially there is expected to be a central region with coexisting solid and liquid phases, surrounded by a hot solid zone. The outer solid zone accounts for the high-energy peak in the $z(x,y)\bar{z}$ analysis that is absent in the $z(x,x)\bar{z}$ analysis of these crystalline semiconductors.[16] The single $z(x,x)\bar{z}$ peak and the low-energy $z(x,y)\bar{z}$ peak are due to solid silicon and germanium no longer in the [001] orientation, corresponding to randomly oriented solid regions at the melting temperature floating in the molten zone. (Scattering from misoriented recrystallized regions is also possible just above melting threshold.[17]) The decrease in Raman intensity with increasing P is explained by the decreasing fraction of solid material within the partially molten zone, and by noting that molten silicon and germanium have no Raman spectrum.[8] For $P>0.7$ W, the laser-heated zone in germanium is totally molten.

The $z(x,x)\bar{z}$ single peak appears to be only weakly affected by stress.[16] The possible interference between Raman scattering by optical phonons and by laser-created electrons and holes is discussed later in this section.

Haro *et al.*[18] have performed a detailed lattice-dynamical calculation for Raman scattering in Si using anharmonic force constants fit to experiment. The second-order cubic anharmonicity term was used to determine the linewidth Γ, and volume expansion and both the second-order cubic and first-order quartic terms were used to determine the Raman shift Ω. Each of these contributions becomes $\propto T$ at high T. The relatively good agreement with experiment obtained at lower temperatures (<800 K) was an improvement over the earlier shell-model calculation by Cowley.[19] Higher-order terms, starting with the second-order quartic terms which are $\propto T^2$, must also be included for improved agreement of these calculations with experiments at higher temperatures. Narasimhan and Vanderbilt[20] recently obtained similar results for the linewidth variation with T, using a less-empirical determination of anharmonic force constants and a similar perturbative approach. The molecular-dynamics study by Wang *et al.*[21] obtained excellent agreement with the experimental frequency shift and linewidth of optical phonons in Si to 1100 K. Because there are no calculations for Ge and because the Si calculations were not performed near the melting temperature, simple perturbation models based on the three-phonon (cubic) coupling and four-phonon (quartic) coupling are used here to analyze the data.

The decrease of the Raman shift of $q=0$ optical phonons with increasing temperature is due the change of harmonic frequency with volume expansion and anharmonic coupling to phonons of other branches. The real part of the phonon self-energy shift can be written as

$$\Omega(T)=\omega_0+\Delta^{(1)}(T)+\Delta^{(2)}(T)\ , \tag{1}$$

where $\omega_0+\Delta^{(2)}(0)$ is the Raman shift as $T\rightarrow 0$ K, $\Delta^{(1)}(T)$ is the thermal-expansion contribution to the line shift, and $\Delta^{(2)}(T)$ is due to anharmonic coupling. $\Delta^{(1)}(T)$ can be written as[1]

$$\Delta^{(1)}(T)=\omega_0\left[\exp\left[-3\gamma\int_0^T\alpha(T')dT'\right]-1\right]\ , \tag{2}$$

where γ is the Grüneisen parameter for the optical Raman mode, 0.98 for c-Si and 1.13 for c-Ge,[22] and $\alpha(T)$ is the coefficient of linear thermal expansion.[23]

The correction of the self-energy due to anharmonic coupling can be modeled as

$$\Delta^{(2)}(T)=C\left[1+\frac{1}{(e^{x_1}-1)}+\frac{1}{(e^{x_2}-1)}\right]+D\left[1+\frac{3}{(e^{y}-1)}+\frac{3}{(e^{y}-1)^2}\right]\ , \tag{3}$$

where the first term corresponds to coupling the optical phonon to two identical ($x_1=x_2$) or different ($x_1\neq x_2$) phonons and the second term corresponds to coupling to three identical phonons. The notation used here closely follows that of Ref. 2.

Similarly, the Raman linewidth can be modeled as[1,2]

TABLE I. Comparison of experiment and model prediction of the Raman shift (Ω) and linewidth (Γ) at the melting temperature in Si (1690 K). The fits are obtained using data from Refs. 1 and 2, with ω_0 fixed at 528.0 cm^{-1}.

Model No.	Model	A (cm^{-1})	B (cm^{-1})	C (cm^{-1})	D (cm^{-1})	Ω 1690 K	Γ 1690 K
I	Klemens [$\Delta^{(1)}(T)\equiv 0$]	1.3200	0.0	−3.500	0.0	496.7	11.8
II	Klemens [$\Delta^{(1)}T\neq 0$]	1.3200	0.0	−3.500	0.0	487.5	11.8
III	Menendez-Cardona [$\Delta^{(1)}(T)\neq 0$]	1.3200	0.0	−3.500	0.0	484.4	12.9
IV	Menendez-Cardona + four-phonon term [$\Delta^{(1)}(T)\neq 0$]	1.2254	0.0946	−3.485	−0.015	482.6	24.7
V	Balkanski [$\Delta^{(1)}(T)\equiv 0$]	1.2130	0.1070	−3.356	−0.144	478.7	25.2
VI	Balkanski [$\Delta^{(1)}(T)\neq 0$]	1.2130	0.1070	−3.450	−0.050	481.2	25.2
	Experiment: Ref. 8					480±2	28
	Experiment + model: Ref. 24 (1673 K)					478.9	25.3
	Experiment: This work					481.7 ±0.4	24.3 ±0.3

$$\Gamma(T)=A\left[1+\frac{1}{(e^{x_1}-1)}+\frac{1}{(e^{x_2}-1)}\right]+B\left[1+\frac{3}{(e^{y}-1)}+\frac{3}{(e^{y}-1)^2}\right]. \quad (4)$$

This linewidth is usually equal to the phonon damping rate, which is the imaginary part of the phonon self-energy. When the real part of the self-energy changes rapidly with frequency, which is not expected here, there is an additional contribution to the linewidth.[1] This model for the linewidth includes phonon decay into two identical or different phonons (three-phonon process) and into three identical phonons (four-phonon process) and is similar to Eq. (3). Above the Debye temperature, the first terms in Eqs. (3) and (4) are linear in temperature, while the second terms are quadratic.

Klemens[6] considered the coupling of the optical phonon with frequency ω_0 to two phonons of equal frequency $\omega_0/2$ [$x_1=x_2=\hbar\omega_0/2k_BT$ and $B=D=0$ in Eqs. (3) and (4)] and did not include the thermal-expansion term. (This is called model I in Tables I and II and Figs. 2–5. When thermal expansion is included for Ω, it becomes model II.) Balkanski *et al.*[2] improved the fit of Ω and Γ obtained from Si Raman spectra at high T by adding the second term in Eqs. (3) and (4), which includes coupling to three phonons with equal frequency $\omega_0/3$($y=\hbar\omega_0/3k_BT$). Again, the effect of thermal expansion was not included in the analysis (model V). Inclusion of thermal expansion (model VI) decreases the value of D in Eq. (3); that is, the four-phonon process appears to become less important. Menendez and Cardona[1] noted the importance of thermal expansion in determining Ω for Si and Ge, but they did not compare their model with experimental Raman shifts. In their discussion of the Raman linewidth, they also noted that in coupling the $q=0$ optical phonon to two phonons, the most important contribution need not be to two identical phonons. They claimed that for Ge and Si the highest final joint density of states occurs when these two phonons are from different branches (LA and LO) and have different frequency,[1] leading to $x_1=0.35\hbar\omega_0/k_BT$ and x_2

TABLE II. Comparison of experiment and model prediction of the Raman shift (Ω) and linewidth (Γ) at the melting temperature in Ge (1210 K). The fits are obtained using data from Ref. 1, with ω_0 fixed at 306.2 cm^{-1}.

Model No.	Model	A (cm^{-1})	B (cm^{-1})	C (cm^{-1})	D (cm^{-1})	Ω 1210 K	Γ 1210 K
I	Klemens [$\Delta^{(1)}(T)\equiv 0$]	0.7500	0.0	−1.200	0.0	293.0	8.3
II	Klemens [$\Delta^{(1)}(T)\neq 0$]	0.7500	0.0	−1.200	0.0	285.4	8.3
III	Menendez-Cardona [$\Delta^{(1)}(T)\neq 0$]	0.7500	0.0	−1.200	0.0	284.1	9.1
IV	Menendez-Cardona + four-phonon term [$\Delta^{(1)}(T)\neq 0$]	0.7352	0.0148	−1.198	−0.002	283.8	11.9
V	Balkanski [$\Delta^{(1)}(T)\equiv 0$]	0.7283	0.0217	−1.132	−0.068	279.8	12.5
VI	Balkanski [$\Delta^{(1)}(T)\neq 0$]	0.7283	0.0217	−1.187	−0.013	282.9	12.5
	Experiment:					281.4	14.1
	This work					±0.5	±0.5

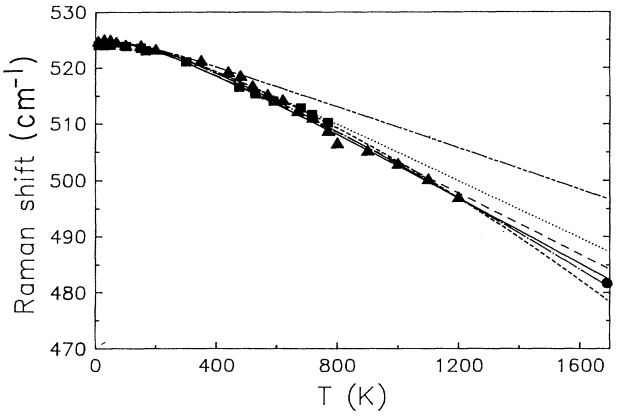

FIG. 2. Raman shifts of Si as a function of temperature, fit using models I–VI. Data reproduced from Ref. 1 are the squares; data from Ref. 2 are the triangles. The shift at the melting temperature obtained in this work is the circle at 1690 K. The fitting curves, from top to bottom at 1690 K, are model I (–··–··), II (· · · ·), III (— — — —), IV (——), VI (–·–·), and V (- - -). Models I–VI are defined in the text and in Table I.

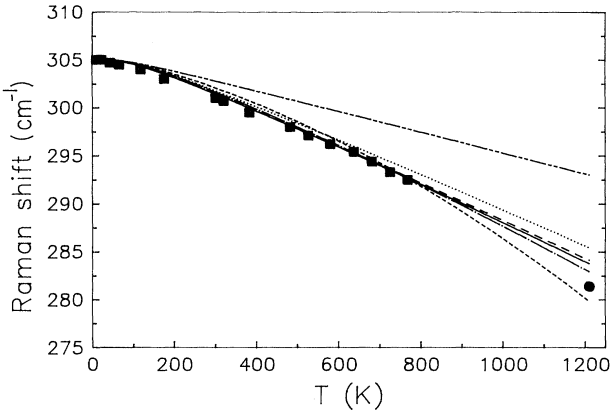

FIG. 4. Raman shifts of Ge as a function of temperture, fit using models I–VI. Data reproduced from Ref. 1 are the squares. The shift at the melting temperature obtained in this work is the circle at 1210 K. The curves, from top to bottom at 1210 K, are model I (–··–··), II (· · · ·), III (— — — —), IV (——), VI (–·–·–·), and V (- - -). Models I–VI are defined in the text and in Table II.

$=0.65\hbar\omega_0/k_BT$ in Eqs. (3) and (4) ($B=D=0$) (model III). The calculations of Narasimhan and Vanderbilt[20] suggest that coupling to pairs of LA-LO phonons does not occur, but that model III is still reasonable because coupling to pairs of LA-TA phonons near the edges of the Brillouin zone is very important. At high temperatures, coupling to three phonons, possibly with different frequencies, can be included. (With coupling to three identical phonons, this is model IV.)

In Table I and Figs. 2 and 3, comparison is made between the Raman parameters measured here and by Nemanich *et al.*[8] for Si at the melting point $T_m=1690$ K, and data from earlier studies conducted at lower temperatures.[1,2] The Raman shift at 1690 K measured here is very close to that measured in Ref. 8, though the linewidth measured here is significantly smaller. Also listed in Table I are values that Compaan *et al.*[24] deduced for 1673 K from their study of pulsed laser heating (with no melting), after their Raman data were deconvoluted to account for temperature nonuniformity. The

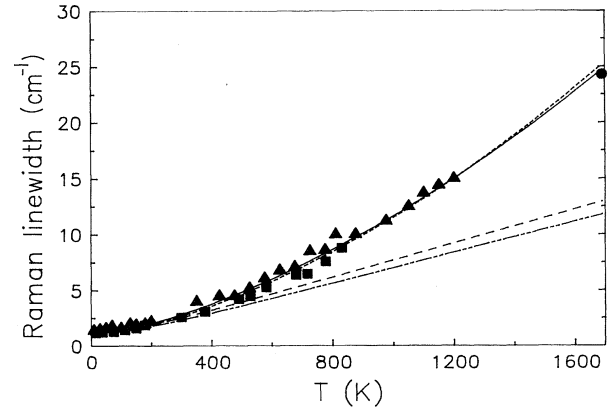

FIG. 3. Raman linewidth of Si as a function of temperature, fit using models I–VI. Data reproduced from Ref. 1 are the squares; data from Ref. 2 are the triangles. The linewidth at the melting temperature obtained in this work is the circle at 1690 K. The curves, from bottom to top at 1690 K, are model I (–··–··), III (— — — —), IV (——), and V (- - -). Models I–VI are defined in the text and in Table I. Note that the linewidths are identical for models I and II, and also for models V and VI.

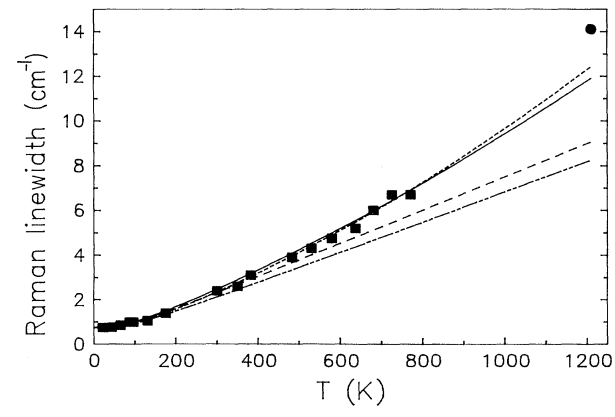

FIG. 5. Raman linewidth of Ge as a function of temperature, fit using models I–VI. Data reproduced from Ref. 1 are the squares. The linewidth at the melting temperature obtained in this work is the circle at 1210 K. The fitting curves, from bottom to top at 1210 K, are model I (–··–··), III (— — — —), IV (——), and V (- - -). Models I–VI are defined in the text and in Table II. Note that the linewidths are identical for models I and II, and also for models V and VI.

data from Refs. 1 and 2 were fit by using models I–VI and then the fits were extrapolated to T_m. Note that for the linewidths, models I and II are identical and so are models V and VI. The value of ω_0 has been fixed at 528.0 cm^{-1}, which is the value from Ref. 2. In three-phonon coupling ($B=D=0$), A and C are determined using the lowest temperature points in Refs. 1 and 2. When four-phonon coupling is also included, B and D are chosen to get a good fit near 1200 K. (Note that small differences in model extrapolations to T_m may be due to details of the fitting procedure.)

When thermal expansion is neglected, the Klemens three-phonon model (model I) gives a poor fit of the Raman shift, while a good fit is obtained when the four-phonon term (from Balkanski *et al.*,[2] model V) is added (Fig. 2 and Table I). Inclusion of thermal expansion improves the three-phonon models (II and III), giving a satisfactory fit with the Menendez-Cardona model (III). When the four-phonon term is also added to the Klemens (VI) or Menendez-Cardona (IV) three-phonon model, very good fits to the lower temperature and melting temperature data are obtained. Note that in models IV, V, and VI, the amplitude of the four-phonon term D is always negative and its magnitude decreases with model refinement, even though the $\Omega(T_m)$ prediction remains essentially the same: first with the inclusion of thermal expansion (model V to VI) and then with the improved three-phonon term (model VI to IV).

As seen in Fig. 3, inclusion of the four-phonon term is necessary to model the Raman linewidth in silicon. The extrapolation of the low-temperature data to the melting point agrees well with the linewidth measured here.

A similar comparison of the Raman parameters is made in Table II and Figs. 4 and 5 for Ge. Equations (1)–(4) are used to extrapolate the lower-temperature experimental data from Ref. 1 to $T_m=1210$ K. A, B, C, and D are chosen in a way similar to that used for Si, with $T\sim750$ K data used to determine B and D. The linewidth fit is insensitive to the choice of ω_0, while the fit of the Raman shift is very sensitive to ω_0 because $\Omega(T=0)=\omega_0+C+D$ [from Eqs. (1) and (3)]. Figure 4 has been plotted with $\omega_0=306.2$ cm^{-1}. Increasing ω_0 to 306.3 cm^{-1} almost eliminates the four-phonon term in model VI, with D changing from -0.013 to -0.005 cm^{-1}. Decreasing ω_0 to 306.0 cm^{-1} changes D to -0.029 cm^{-1}. This last modification leads to a slightly poorer fit at lower temperature and a large splitting (3 cm^{-1}) between the model III and VI predictions of $\Omega(T_m)$. Models III–VI all give fair fits to the Raman shift data in Ge.

The Raman linewidth in Ge extrapolated to the melting point is 6 cm^{-1} smaller than the present measurement when only three-phonon coupling is included. The measured linewidth is within ~2 cm^{-1} of the extrapolation when four-phonon coupling is also included.

Though it is not possible to uniquely fit the data in Figs. 2–5 with these models, some points are clear. In fitting the Raman linewidth in Si and Ge, terms both linear and quadratic in temperature are necessary. In contrast, the linear terms alone, including that due to volume expansion, provide an adequate fit to the Raman shift data, while the quadratic terms make only a small correction needed for temperatures near the melting point.

The connection of the models used here to analyze the Raman spectra and the anharmonic potential should be clarified.[2,18] Both the self-energy correction in Eq. (3) and the linewidth in Eq. (4) have been described as the sum of two terms, the first term couples the optical phonon to two phonons and the second term couples it to three phonons. Above the Debye temperature, they vary as $\sim T$ and $\sim T^2$, respectively. For $\Gamma(T)$, this model of phonon decay corresponds closely with theory. The two terms in Eq. (4) correspond to cubic and quartic terms in the potential, respectively, both in second-order perturbation. For $\Delta^{(2)}(T)$, the correspondence between the model and each term in the anharmonic potential is less direct. Second-order cubic and first-order quartic terms both have the linear temperature dependence at high T exhibited by the first term in Eq. (3). The cubic term couples the optical phonon to two lower-energy phonons as in the model, while the quartic term is a renormalization based on the creation and annihilation of a phonon, and does not directly relate to a term in the model. Second-order quartic terms and other higher-order terms exhibit the quadratic temperature dependence of the second term in Eq. (3). One of these second-order terms corresponds to the coupling of the optical phonon to three lower-energy phonons, as in the model.

The possible interference between Raman scattering by optical phonons and by laser-created electrons and holes, known to produce a Fano-like line shape, should be considered before concluding this discussion. It is difficult to assess the importance of free carriers in this experiment, even though there have been detailed Raman studies of doped Si and Ge at 77 and 300 K.[25] Past work has shown that as the continuum electronic scattering becomes more important, the Raman profile typically shifts down in frequency and broadens, eventually becoming asymmetric and then very distorted.[25] In both Si and Ge, electronic scattering of holes is much more important than that of electrons. At 77 and 300 K, hole densities of $\sim2\times10^{20}/cm^3$ produced by dopants broaden and downshift the Raman peak by ~5–20 cm^{-1} in these semiconductors (5145 Å).[25]

An upper limit for the steady-state density of electrons and holes during laser irradiation is estimated by balancing carrier creation by photon absorption and loss by Auger recombination,[7] giving $\sim5\times10^{20}/cm^3$ at the center of the spot at the surface for both Si and Ge. This peak value is over an order of magnitude larger than the free-carrier density for each semiconductor at the melting temperature (unirradiated),[7] and may well be an overestimate because it neglects diffusion and the effect of the nearby conducting, molten regions. The Raman measurements made at lower temperature cannot be used at 1690 K because the band structure is very different near T_m. For instance, in Si the band gap of the direct transition E_0' decreases from 3.3 to ~2.6 eV as T increases from 300 to 1690 K.[26] Because of resonance effects, this

change should decrease the importance of electronic scattering relative to phonon scattering at T_m.[27] Also, the exact shapes of the heavy- and light-hole bands at 1690 K, which critically affect the scattering of holes, are not known. Furthermore, the probability that there is a hole in the initial scattering state but not in the final state decreases by a factor of ~ 2 from 300–1690 K, which would again tend to lessen the relative importance of electronic Raman scattering at 1690 K. In the Raman study of pulsed laser-heated Si, Compaan *et al.*[24] estimated an electron-hole pair density of $\sim 2\times 10^{20}/\text{cm}^3$, but found that their $T = 600-1400\,^{\circ}\text{C}$ data were well modeled assuming a much lower density $\sim 2\times 10^{19}/\text{cm}^3$ (and the 300 K parameters). This lower density would lead to a decrease of Ω by $< 0.5\ \text{cm}^{-1}$ and an increase of Γ by $\sim 2\ \text{cm}^{-1}$.

In Ref. 8, heating was provided by light with energy below the Si band gap, so no free carriers were created by photon absorption. If carrier effects were important here, a smaller shift and a broader linewidth would have been measured in this study. The frequency shifts measured here and in Ref. 8 in Si are effectively the same, while the linewidth measured here is in fact smaller. Also, no change in the Raman shift or width and no asymmetry was seen for Si or Ge over the range of laser power and corresponding carrier density ($\sim P^{1/3}$) examined here. Small changes would be measurable if the high carrier densities estimated here were accurate (assuming the parameters at 300 K). Note that in Ge the experimental frequency and linewidth data are $\sim 1-2\ \text{cm}^{-1}$ below and above model predictions at T_m, respectively. One cannot rule out the possibility that these differences are due to a small free-carrier effect.

IV. CONCLUDING REMARKS

Coupling of the optical phonons produced in Raman scattering both to two and to three phonons is needed to describe optical-phonon decay up to the melting temperature in both silicon and germanium. Three-phonon processes and volume expansion, which both have a linear temperature dependence, are very important in determining anharmonic contributions to the real part of the phonon self-energy and can fit the Raman shift dependence on temperature very well. Terms with a quadratic temperature dependence above the Debye temperature, such as the coupling of an optical phonon to three lower-energy phonons, seem to have a less significant effect on the Raman shift.

ACKNOWLEDGMENTS

The authors would like to acknowledge support by the Office of Naval Research and IBM, and to thank J. A. Tuchman and P. Leong for assistance in data analysis, D. Biegelsen, G. Olson, R. Lemons, and H. van Driel for discussions about laser heating and melting of silicon, and J. Tsang and A. Compaan for discussions on photocreated electrons and holes.

[1] J. Menendez and M. Cardona, Phys. Rev. B **29**, 2051 (1984).
[2] M. Balkanski, R. F. Wallis, and E. Haro, Phys. Rev. B **28**, 1928 (1983).
[3] R. Tsu and J. G. Hernandez, Appl. Phys. Lett. **41**, 1016 (1982).
[4] H. W. Lo and A. Compaan, J. Appl. Phys. **51**, 1565 (1980).
[5] T. R. Hart, R. L. Aggarwal, and B. Lax, Phys. Rev. B **1**, 638 (1970).
[6] P. G. Klemens, Phys. Rev. **148**, 845 (1966).
[7] G. D. Pazionis, H. Tang, and I. P. Herman, IEEE J. Quantum Electron. **25**, 976 (1989).
[8] R. J. Nemanich, D. K. Biegelsen, R. A. Street, and L. E. Fennell, Phys. Rev. B **29**, 6005 (1984).
[9] J. S. Preston, H. M. van Driel, and J. E. Sipe, Phys. Rev. Lett. **58**, 69 (1987), and references cited therein.
[10] K. A. Jackson and D. A. Kurtze, J. Cryst. Growth **71**, 385 (1985).
[11] W. G. Hawkins and D. K. Biegelsen, Appl. Phys. Lett. **42**, 358 (1983).
[12] R. A. Lemons and M. A. Bosch, Appl. Phys. Lett. **40**, 703 (1982).
[13] H. E. Cline, J. Appl. Phys. **52**, 443 (1981).
[14] R. A. Lemons and M. A. Bosch, Appl. Phys. Lett. **39**, 343 (1981).
[15] E. Anastassakis and Y. S. Raptis, J. Appl. Phys. **57**, 920 (1985).
[16] H. Tang and I. P. Herman (unpublished).
[17] M. Combescot, J. Bok, and C. Benoit à la Guillaume, Phys. Rev. B **29**, 6393 (1984).
[18] E. Haro, M. Balkanski, R. F. Wallis, and K. H. Wanser, Phys. Rev. B **34**, 5358 (1986).
[19] R. A. Cowley, J. Phys. (Paris) **26**, 659 (1965).
[20] S. Narasimhan and D. Vanderbilt, in *Phonons 89, Proceedings of the Third International Conference on Phonon Physics and the Sixth International Conference on Phonon Scattering in Condensed Matter,* edited by S. Hunklinger, W. Ludwig, and G. Weiss (World Scientific, Singapore, 1990), p. 211.
[21] C. Z. Wang, C. T. Chan, and K. M. Ho, Phys. Rev. B **40**, 3390 (1989).
[22] B. A. Weinstein and G. J. Piermarini, Phys. Rev. B **12**, 1172 (1975).
[23] *Thermophysical Properties of Matter,* edited by Y. S. Touloukian and R. K. Kirby (Plenum, New York, 1975), Vol. 12, p. 116; *ibid.* Vol. 13, p. 155 (1977).
[24] A. Compaan, M. C. Lee, and G. J. Trott, Phys. Rev. B **32**, 6731 (1985).
[25] G. Abstreiter, M. Cardona, and A. Pinczuk, in *Light Scattering in Solids IV,* edited by M. Cardona and G. Guntherodt (Springer, Berlin, 1984), p. 5.
[26] G. E. Jellison, Jr. and F. A. Modine, Phys. Rev. B **27**, 7466 (1983).
[27] F. Cerdeira, T. A. Fjeldly, and M. Cardona, Phys. Rev. B **8**, 4734 (1973).